


## Research Article

# Evaluation of the Corrosion Inhibiting Capacity of Silica/Polypyrrole-Oxalate Nanocomposite in Epoxy Coatings

Van T. H. Vu,<sup>1,2</sup> Thanh T. M. Dinh ,<sup>1,2,3</sup> Nam T. Pham,<sup>1</sup> Thom. T. Nguyen,<sup>1</sup> Phuong T. Nguyen,<sup>1</sup> and Hang T. X. To<sup>1</sup>

<sup>1</sup>Institute for Tropical Technology, Vietnam Academy of Science and Technology, 18 Hoang Quoc Viet, Cau Giay District, Hanoi, Vietnam

<sup>2</sup>Graduate University of Science and Technology, Vietnam Academy of Science and Technology, 18 Hoang Quoc Viet, Cau Giay District, Hanoi, Vietnam

<sup>3</sup>University of Science and Technology of Hanoi, Vietnam Academy of Science and Technology, 18 Hoang Quoc Viet, Cau Giay District, Hanoi, Vietnam

Correspondence should be addressed to Thanh T. M. Dinh; [dmthanh@itt.vast.vn](mailto:dmthanh@itt.vast.vn)

Received 23 May 2018; Accepted 31 July 2018; Published 2 September 2018

Academic Editor: Flavio Deflorian

Copyright © 2018 Van T. H. Vu et al. This is an open access article distributed under the Creative Commons Attribution License, which permits unrestricted use, distribution, and reproduction in any medium, provided the original work is properly cited.

Silica/Polypyrrole nanocomposites ( $\text{SiO}_2/\text{PPy}$ ) incorporating oxalate as counter anion ( $\text{SiO}_2/\text{PPyOx}$ ) were chemically polymerized in the solution with the presence of pyrrole, silica, and sodium oxalate. Nanocomposites  $\text{SiO}_2/\text{PPyOx}$  at different concentrations of oxalate anion were characterized with FTIR, XRD, EDX, TGA, and TEM. The corrosion protective properties for carbon steel of nanocomposites in epoxy coating were studied by electrochemical techniques including electrochemical impedance spectroscopy (EIS) and open circuit potential (OCP). FTIR results of nanocomposites show a slightly red-shift in terms of wavelength compared with the case of PPy and  $\text{SiO}_2$  spectra. It may be due to a better conjugation and interactions between PPy and  $\text{SiO}_2$  in nanocomposite structure. TEM image indicated that nanocomposites have spherical morphologies with diameters between 100 and 150 nm. The EIS results showed that  $|Z|$  modulus values of epoxy coatings containing  $\text{SiO}_2/\text{PPyOx}$  composites reached about  $10^{9.7} \Omega \cdot \text{cm}^2$ , always higher than that of epoxy coating. These results are also confirmed by OCP results. It proves that the presence of oxalate anion can enhance the resistance against corrosion and it has been shown that the content of counter anion strongly affects the anticorrosion ability.

## 1. Introduction

Conventional polymer coating like epoxy is well known to have superior characteristics as compared to regular paints due to its good scratch resistance and strong adhesion to metal surface [1, 2]. However, over time, the barrier coating can fail due to prolonged exposure to the environment. At the interface between the metal and an aqueous medium, there are two spontaneous coupled reactions. One is the oxidation reaction on metal surface. The electrons from metal are removed by the chemical species from the aqueous environment; the other is the participation of metal surface atoms to replenish the electron deficiency. Corrosion control based on organic coatings is mainly classified into three systems: electrochemical inhibitors, cathodic protection, and

barrier coatings. The chromates-based metallic coatings are widely used to protect metal from corrosion by passivating the metal surface. But nowadays, it is limited by the governmental policy because the hexavalent chromium is known as carcinogen chemical [3]. The cathodic protection is offered by sacrificial coatings, such as zinc rich epoxies, but the only drawback of this technique is that a large amount of zinc is required to prolong the metal life time, which leads to an adherence loss, a high solid content, and porosity in the paint. The last system, barrier coatings have numerous advantages such as low cost and the ease of preparation, and a wide range of products is available.

Some recent results have shown that the presence of nanoparticles in epoxy coating can increase the mechanical and thermal properties as well as the corrosion resistance

of the coating [4–6]. In terms of high surface area, good dispersion, ease of preparation, and improved chemical and thermal stabilities, nanosilica is a potential candidate among the inorganic oxides [7, 8].

In the late 70s, Heeger, Shirakawa, and MacDiarmid discovered that Polyacetylene can transport electrical charges along its chains. A few decades later, they have been awarded the Nobel Prize in Chemistry for their discovery and development of conductive polymers [9–11]. This opens a new class of materials to be explored. Intrinsic Conductive Polymers (ICP) can combine the electronic and optical properties of semiconductors and metals with the mechanical properties and ease of processing associated with polymers. Among ICPs, polypyrrole (PPy) is widely used due to its unique properties such as environmental stability, high conductivity, and anticorrosion ability [12–15]. The researches in PPy's applications are focusing on the use of PPy film for a protective coating or anticorrosion additives organic coatings [13, 16–20]. Nanosilica particles are incorporated inside the matrix of conducting polymer in order to form a core-shell structure of ICPs-Silica, which results in the increase of the active area surface of the conducting polymer, compared to its bulk form.

On the whole, there are clear evidences that PPy provides corrosion protection for steel [13–20]. Besides this, several operating corrosion protection mechanisms have been proposed, such as barrier protection, corrosion inhibition, and anodic protection. It has been suggested that anodic protection, a shift in corrosion potential from the active region to passive one, can explain the protective capacity of PPy toward steel [18–20]. But the maintenance of PPy protective ability alone is limited. During the synthesis of PPy, counter anions can be incorporated into PPy matrix by neutralizing the positive charges on the polymer backbone. Counter anions play an important role in the change of physical properties and morphology [21]. Small anions can be released from the polymer coating and provide some additional protection when the coating is reduced [16, 22, 23].

Grari et al. have shown that multilayered polypyrrole-silica coating can improve the corrosion protection for stainless steel by electrophoretic deposition [24]. G. Ruhi et al. indicated that chitosan-polypyrrole-SiO<sub>2</sub> can enhance thermal stability and anticorrosive properties for epoxy coating [25]. There are some studies subjecting the use of counter anions with polypyrrole [21, 26–28]. However, there is no study to combine all the advantages such as anticorrosion ability of polypyrrole, the low cost and high stability of silica, and inhibitive property of counter anion. Hence, we report silica/polypyrrole-oxalate (SiO<sub>2</sub>/PPyOx) to use as a corrosion resistance additive in epoxy coating system for carbon steel substrates. Studies are focused to highlight the role of oxalate anions in improving the corrosion resistance properties of silica/polypyrrole composite.

## 2. Materials and Methods

**2.1. Chemicals.** Pyrrole (Merck, 97%) was distilled before use. Tetraethyl orthosilicate (TEOS) was purchased from Daejung, South Korea, 98%; hydrogen chloride (HCl, 36.5%),

iron (III) chloride hexahydrate (FeCl<sub>3</sub>·6H<sub>2</sub>O, 98%), sodium oxalate (Na<sub>2</sub>C<sub>2</sub>O<sub>4</sub>, 99.5%), acetone (C<sub>3</sub>H<sub>7</sub>O, 99.5%), xylene (C<sub>8</sub>H<sub>10</sub>, 98.5%), and methanol (CH<sub>4</sub>O, 99.5%) were purchased from Huakang, China; epoxy bisphenol A, Epotec YD011-X75, and Polyamide 307D-60 were purchased from Kukdo Chemical Co., Ltd. (South Korea).

**2.2. Preparation of SiO<sub>2</sub>.** 10g TEOS was dropped slowly into 140 ml HCl solution (pH = 1). The mixture was stirred by magnetic stirrer for 24 hours at room temperature and then heated to 80°C for 24 hours. The precipitate was washed and filtered by distilled water to pH=7. Finally, the samples were dried at 80°C for 24 hours in vacuum oven.

**2.3. Preparation of SiO<sub>2</sub>/PPyOx Composites.** 0.15 g of SiO<sub>2</sub> was dispersed in 0.3 M of an aqueous solution of FeCl<sub>3</sub> by using an ultrasonic sonicator for 30 minutes. Different quantity of sodium oxalate solution (1.125 mM, 2.5 mM, and 5 mM) was then added to this mixture and stirred at room temperature for 1 hour and labeled as SPO1, SPO2, and SPO3, respectively. Then 0.01 M of pyrrole was injected slowly in the above mixture for the polymerization of the pyrrole monomer. This process was kept under stirring for 24 hours. Then the synthesized SiO<sub>2</sub>/PPyOx composites were washed with distilled water, and then with a mixture of methanol and acetone (volume ratio 1:1). Finally, the synthesized products were dried at 80°C for 24 hours in a vacuum oven.

**2.4. Preparation of Epoxy Coating.** Carbon steel sheets (150 mm × 100 mm × 2 mm) were used as substrates. These substrates were polished with abrasive papers 80, 240, 320, and 600 grades and cleaned with ethanol. The epoxy resin was epoxy bisphenol A, Epotec YD011-X75; epoxy equivalent weight is about 470 g/eq. Polyamide 307D-60 (equivalent weight per active H is 266 g/eq) was used as the hardener. The composites SiO<sub>2</sub>/PPy, SiO<sub>2</sub>/PPyOx (with 1.125 mM, 2.5 mM, and 5 mM of sodium oxalate in the oxidant solution) were incorporated in epoxy resin at 5 wt% with xylene as solvent and named as ESP, ESPO1, ESPO2, and ESPO3, respectively. The liquid paints were deposited on the bare steel using a spin-coater at rotating speeds up to 1000 rpm. Finally, all samples were dried at ambient temperature for 24 hours.

**2.5. Analytical Characterizations.** Phase identification of synthesized SiO<sub>2</sub>, PPy, and SiO<sub>2</sub>/PPyOx composites was determined by X-ray diffractometer (Shimadzu XRD-6100, Japan, using Cu Kα radiations = 1.5405 Å) with scanning rate 2° per min and 2 theta (2θ) angle ranging from 5° to 80° at current 30.0 mA and voltage 40.0 kV.

The FTIR characterization of composites SiO<sub>2</sub>-PPyOx was carried out by the KBr method on a Nicolet IS10 (Thermo Scientific, USA) spectrometer operated at 8 cm<sup>-1</sup> resolution in the 400–4000 cm<sup>-1</sup> region.

Thermogravimetric analysis (TGA) was performed on a TG 209 F1 Libra (Netzsch, Germany), with a heating rate of 10°C per minute in air.

The particle size and morphology of synthesized SiO<sub>2</sub>/PPyOx composites were obtained by Transmission Electron Microscopy- (TEM-) JEM 1010 (Jeol, USA) operating at

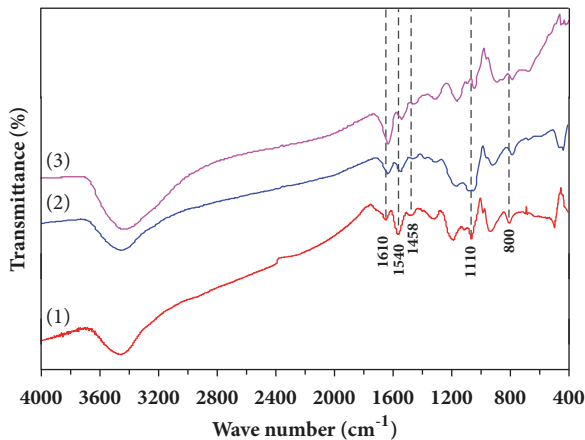


FIGURE 1: FTIR spectra of (1) SPO1, (2) SPO2, (3) SPO3.

80 kV. The energy dispersive X-ray spectrum (EDS) was recorded by an Oxford instrument (model 51-ADD0007, UK).

The dry film thickness of samples was measured by Coating Thickness Gauge (Minitest 600, ElektroPhysik, USA).

**2.6. Electrochemical Measurements.** Protection performance of coatings was evaluated by open circuit potential and electrochemical impedance measurements using a ZIVE MP2A Instrument. A conventional electrochemical system with three-electrode cell with a platinum auxiliary electrode, a saturated calomel reference electrode (SCE), and a coated carbon steel working electrode with an exposed area of 11 cm<sup>2</sup> was used for all electrochemical experiments. Impedance measurements were performed at the 100 kHz–0.01Hz frequency range at OCP by applying a 10 mV sinusoidal potential signal. The corrosive medium was a 3% NaCl solution. Each experiment was done at least three times.

The corrosion resistance of the coating was determined by salt spray test (ASTM B117). In this method, the coating is subjected to a salt spray environment for extended periods of time (up to 28 days) at an elevated temperature (40°C).

### 3. Results and Discussion

**3.1. FT-IR Analysis.** Figure 1 presents the infrared spectra of SiO<sub>2</sub>/PPy synthesized with different quantity of sodium oxalate. The characteristic bands of SiO<sub>2</sub>/PPyOx change slightly with strong attenuation of the peaks in comparison with the spectra of pure PPy and SiO<sub>2</sub>, which suggests that there is the incorporation between silica, polypyrrole, and oxalate anion. The characteristic bands of PPy were observed at higher wavenumbers from 1540 cm<sup>-1</sup> to 1500 cm<sup>-1</sup>, 1458 cm<sup>-1</sup> to 1450 cm<sup>-1</sup>, and 1150 cm<sup>-1</sup> to 1100 cm<sup>-1</sup> with a broad peak at around 800 cm<sup>-1</sup>. It might be due to the presence of metal oxide bond in synthesized compounds [20]. In addition, the characteristic band of oxalate anions is clearly observed at 1610 cm<sup>-1</sup>. It is a clear evidence of the oxalate anion occurrence [16]. Thus, the FTIR results confirm the formation of SiO<sub>2</sub>/PPy composite and the incorporation of oxalate anions in SiO<sub>2</sub>/PPyOx.

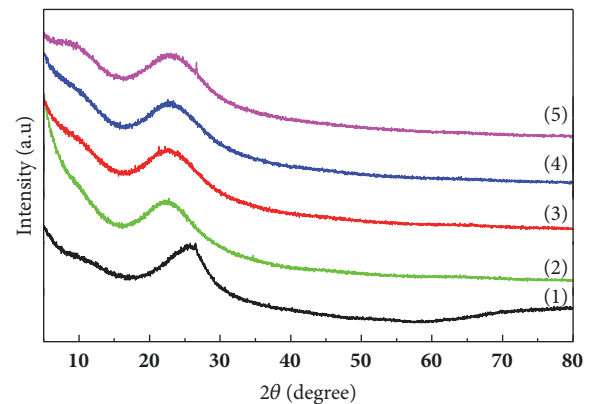
FIGURE 2: XRD patterns of (1) PPy, (2) SiO<sub>2</sub>, (3) SPO1, (4) SPO2, (5) SPO3.

TABLE 1: EDS data of SPO1, SPO2, and SPO3.

	C	O	N	Si
SPO1	34.89	38.64	9.15	17.32
SPO2	34.57	39.29	8.86	17.28
SPO3	35.21	38.69	8.05	18.05

**3.2. X-Ray Diffraction Analysis.** The phase components of pure SiO<sub>2</sub>, PPy, SPO1, SPO2, and SPO3 are shown in Figure 2. Pure PPy has only a broad characteristic peak at  $2\theta=26.5^\circ$ , which indicated its amorphous structure [23]. The diffraction peak at  $2\theta=22.5^\circ$  corresponds to the crystalline nature of synthesized SiO<sub>2</sub> particles. For all synthesized composite samples SPO1, SPO2, and SPO3, the characteristic peak changes insignificantly,  $2\theta=23^\circ$ ; it might be due to the SiO<sub>2</sub> particles embedded in the polymer matrix.

The crystallite size of the composites can be determined from the XRD line-broadening method using the Scherrer equation:

$$D = \frac{0.9\lambda}{\beta \cos \alpha} \quad (1)$$

where D is the average crystallite size,  $\beta$  is the line broadening in radians,  $\alpha$  is Bragg angle,  $\lambda$  is X-ray wavelength.

According to (1), the average crystalline size of composites was found to be approximately 22 nm.

**3.3. The Energy Dispersive X-Ray Spectroscopy (EDX).** The EDX results of SPO1, SPO2, and SPO3 are shown in Figure 3 and summarized in Table 1. Oxygen and silicon are the main elements of silica. The main constituent elements of PPy are carbon and nitrogen. EDX is a straightforward way to indicate the presence of silica in the composites and determine its content. The presence of silicon and oxygen is in agreement with the fact that the SiO<sub>2</sub> was incorporated in PPy. The weight percentages of carbon increase slightly from SPO1 to SPO3; it is due to the increasing concentration of oxalate anion in the initial mixture. Additionally, weight percentages of oxygen fluctuate; it can be explained by the standard deviation of measurement.

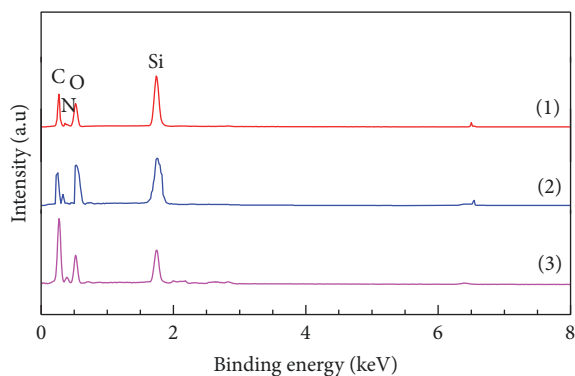


FIGURE 3: EDS spectra of (1) SPO1, (2) SPO2, (3) SPO3.

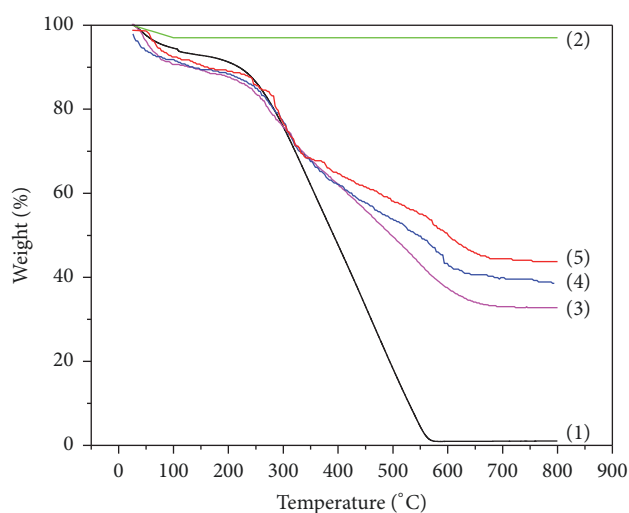


FIGURE 4: TGA curves of (1) PPy, (2) SiO<sub>2</sub>, (3) SPO1, (4) SPO2, (5) SPO3.

**3.4. Thermogravimetric Analysis.** The PPy and SiO<sub>2</sub> content in SPO1, SPO2, and SPO3 composites were determined by TGA (Figure 4). Pure SiO<sub>2</sub> presents a weight loss about 3% below 100°C due to the dehydration of hydrophilic silica surface [29]. On the case of pure PPy, the weight loss occurs from 25 to 100°C which is about 6%. It is well known that PPy is hygroscopic and during the heating to 100°C the residual water evaporates. At temperature between 200 and 570°C, there is a significant weight loss, about 93%, due to the polymer chain degradation. The weight loss of all samples occurs with three different stages. An initial weight loss of 9% (below 100°C) corresponds to the elimination of adsorbed water. After this, a weight loss between 100 and 660°C is about 59%, 51%, and 46% for SPO1, SPO2, and SPO3, respectively. That can be explained by the decomposition of polypyrrole backbone at a high temperature enough. Additionally, SiO<sub>2</sub> and oxalate anions are embedding in the polymer matrix which results in the increase of the thermal decomposition of polypyrrole from 570°C to 660°C. These results can be explained by the high thermal stability of silica; it restricts the thermal motion of polypyrrole chains and shields the

polymer degradation. The remaining weight at 800°C is 31, 38, and 42% with SPO1, SPO2, and SPO3, respectively.

**3.5. TEM.** Figure 5 shows TEM images of synthesized SiO<sub>2</sub>, SiO<sub>2</sub>/PPy, SPO1, SPO2, and SPO3. SiO<sub>2</sub> particles depict spherical morphology with an average diameter of about 40 nm. In the case of SiO<sub>2</sub>/PPy, SPO1, SPO2, and SPO3, the particles size in diameter is higher than that of pure silica and there are agglomerations. It may be due to the pyrrole monomer adsorbed onto the silica surface, and then it was polymerized in the presence of the oxidizing agent (FeCl<sub>3</sub>). Hence, the diameters of nanocomposites particles are increased. It is still a big challenge to make the uniform dispersion of silica into polypyrrole matrix due to the hydrophilic interaction of oxide nanoparticles leading to agglomerates. Various experiments with the different concentration of oxalate anion were attempted for the optimization. However, the size of synthesized nanocomposites has just changed insignificantly (100-150 nm).

**3.6. OCP.** Open circuit potential of carbon steel plates coated with epoxy coating (EP), epoxy coating containing 5 wt% of composites SiO<sub>2</sub>/PPy (ESP), SPO1 (ESPO1), SPO2 (ESPO2), and SPO3 (ESPO3) were measured against time in 3% NaCl solution. Figure 6 shows the variation of OCPs with time for different samples.

The trend of OCP variation for epoxy coating exhibited a gradual shift of potential toward negative direction, from -0.300 V<sub>SCE</sub> to -0.540 V<sub>SCE</sub> after 35 days of immersion. This is probably due to the occurrence of some surface phenomenon, such as the ingress of chloride ions through the coating.

In the case of ESP, the initial potential value of OCP is -0.058 V<sub>SCE</sub>, which is higher than epoxy coating. It can be explained by the effect of PPy in the formation of a passive layer on steel substrate. But the OCP variations dropped to -0.172 V<sub>SCE</sub> after 1 day of immersion. It is attributed to the sudden rapid diffusion of chloride ions through the coating. Then, OCP values reached -0.283 V<sub>SCE</sub> after 35 days of immersion.

In the presence of the SiO<sub>2</sub>/PPyOx composites, the OCP values are significantly increased. At the beginning of the immersion process, the maximum potential values of ESPO1, ESPO2, and ESPO3 are 0.200 V<sub>SCE</sub>, 0.310 V<sub>SCE</sub>, and 0.250 V<sub>SCE</sub>, respectively. It indicates that these coatings provide a large ennoblement and high performance on corrosion. After 10 days of immersion, the OCP values gradually decreased toward negative potential and reached -0.150 V<sub>SCE</sub>, 0.150 V<sub>SCE</sub>, and -0.090 V<sub>SCE</sub> for ESPO1, ESPO2, and ESPO3, respectively. The decline of potential values indicated that diffusion of electrolyte and corrosive ions took place through pinholes which existed in the coating. However, the OCP values increase again till the attainment of a steady state value (0.020 V<sub>SCE</sub>, 0.190 V<sub>SCE</sub>, and -0.011 V<sub>SCE</sub> for ESPO1, ESPO2, and ESPO3, respectively) after 21 days and ones maintained after 35 days of immersion. This phenomenon is due to the triple corrosion protection of SiO<sub>2</sub>/PPyOx composite in epoxy coatings on the underlying steel. On one hand, the composites can improve the physical barrier ability for epoxy coating. On the other hand, when the samples are in contact



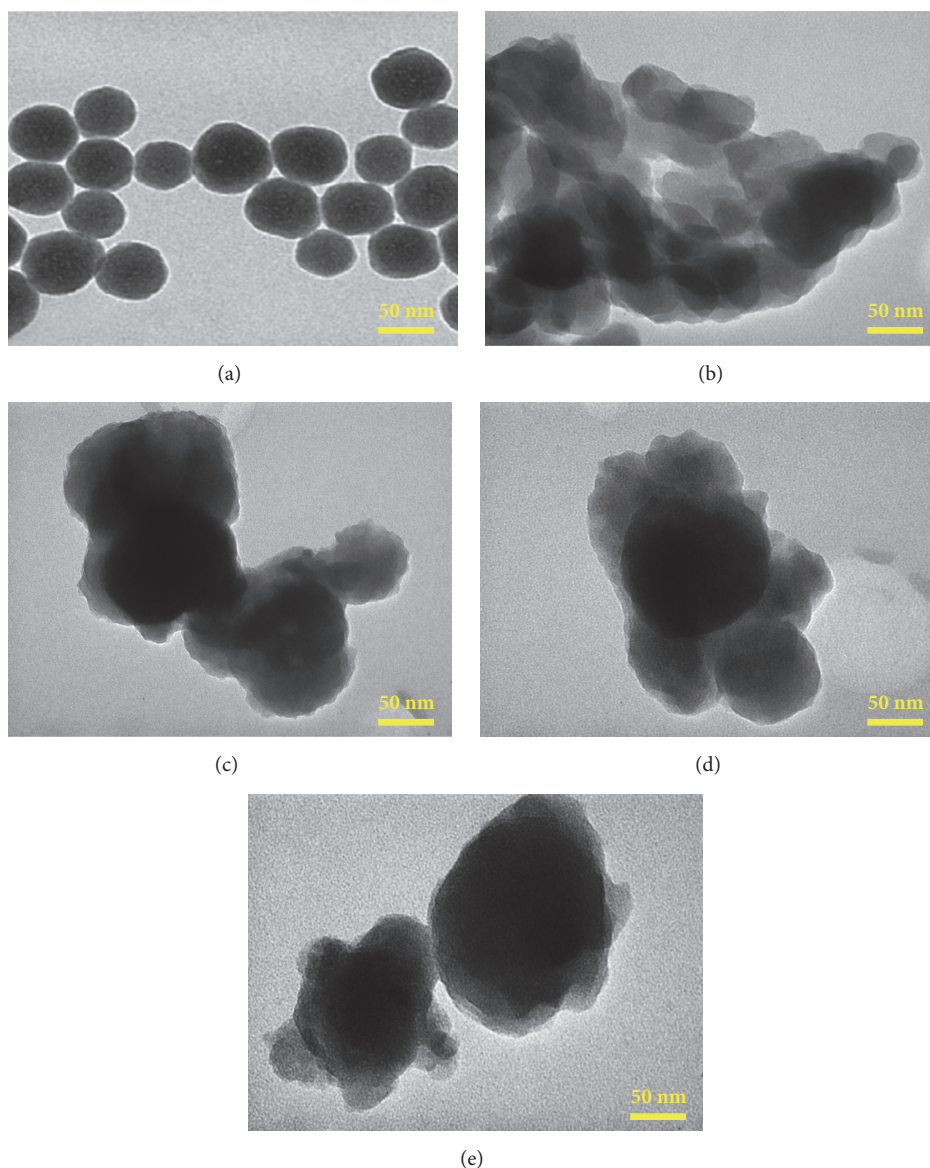


FIGURE 5: TEM images of (a) SiO<sub>2</sub> (b) SiO<sub>2</sub>/PPy, (c) SPO1, (d) SPO2, (e) SPO3.

with the electrolyte solution, an interaction between PPy and iron takes place and results in PPy reduction and Fe oxidation to form its oxide. At the same time, when PPy<sub>emeraldine salt</sub> was converted to PPy<sub>leucoemeraldine base</sub>, oxalate anions which are present as counter anions can be released and become available at the interface between substrate and the coating, which lead to the formation of a passivated layer.

**3.7. EIS.** For further study of corrosion protection performance of epoxy coating and epoxy coating containing 5% composites SiO<sub>2</sub>/PPy, SiO<sub>2</sub>/PPyOx on the coated steel, EIS technique was used to determine the protective properties. Figures 7, 8, and 9 show the Bode plots of different coatings after 1 hour, 14 days, and 35 days of exposure period in a 3% NaCl solution, respectively. Bode plots give simultaneous measurement of modulus of impedance  $|Z|$  and phase angle with respect to frequency.

Figures 7(a) and 7(b) illustrate the Bode plots of all the coatings samples at the beginning of the study. Initially, the impedance value of epoxy coating is  $6.42 \times 10^5 \Omega \cdot \text{cm}^{-2}$ , while by addition of SiO<sub>2</sub>/PPy and SiO<sub>2</sub>/PPyOx composites, impedance values increase significantly. For instance, in the case of ESP, ESPO1, ESPO2, and ESPO3, impedance values were  $1.01 \times 10^7$ ,  $1.02 \times 10^8$ ,  $5.01 \times 10^9$ , and  $2.69 \times 10^9 \Omega \cdot \text{cm}^{-2}$ , respectively.

Bode plots of all the coatings after 14 and 35 days of immersion are shown in Figures 8 and 9. The impedance values of all the samples decreased after a longer exposure time. Epoxy coating, with the presence of polar groups in the structure which is chemically bonded to steel surface, is well known for high adhesive strength. After long immersion time, the interfacial bonding between epoxy and steel surface is destroyed because of the entry of electrolyte into the coating. These results are in the failure of the coating. Silica

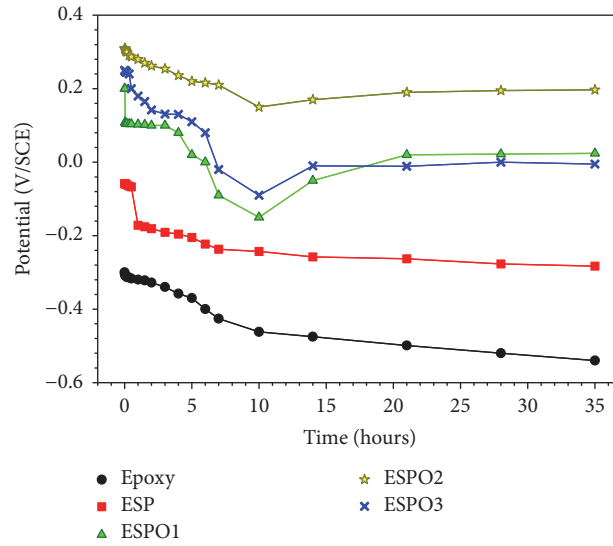


FIGURE 6: Open circuit potential of coated steel samples during immersion time in 3% NaCl solution.

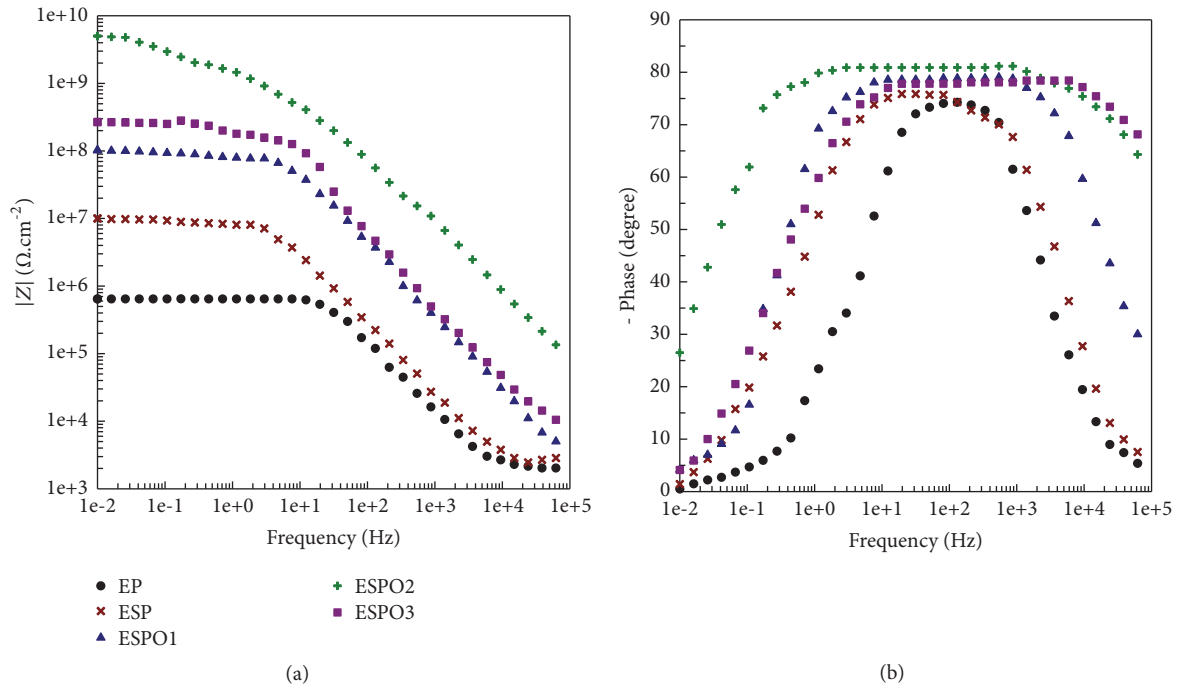


FIGURE 7: Bode plots of coatings after 1 hour of immersion in a 3% NaCl solution.

nanoparticles act as a reinforcing material which enhances the mechanical integrity of the coating. PPy, with its strong oxidative property, works as an oxidant to the steel surface and shifts the steel potentials to passive zone.

The barrier property of a surface coating can be investigated by the impedance magnitude in low frequency region. ESPO1, ESPO2, and ESPO3 showed the high magnitude of impedances in this region, which imply high pore resistance toward the electrolyte diffusion. It indicated that the presence of the  $\text{SiO}_2/\text{PPyOx}$  composite also increases the barrier protective ability for epoxy coating. The most interesting result is ESPO2, because  $|Z|$  value only decreases about 10

times from the beginning to the end of immersion. The important changes in the shape of the Bode plot are respected to a function of exposure and the extended durability of the materials as demonstrated by the maintenance of high  $Z$  values at low frequency up to 35 days. After 1 hour of immersion, the impedance increases from high frequencies to low frequencies. But after a longer immersion time, the Bode plots show capacitive nature (increased impedance) beginning at high frequencies with a break point at approximately 1 Hz, then resistive nature. However, the data from high and low frequency regions are always the highest value compared to other coatings. The phase angle of ESPO2 shows a wide

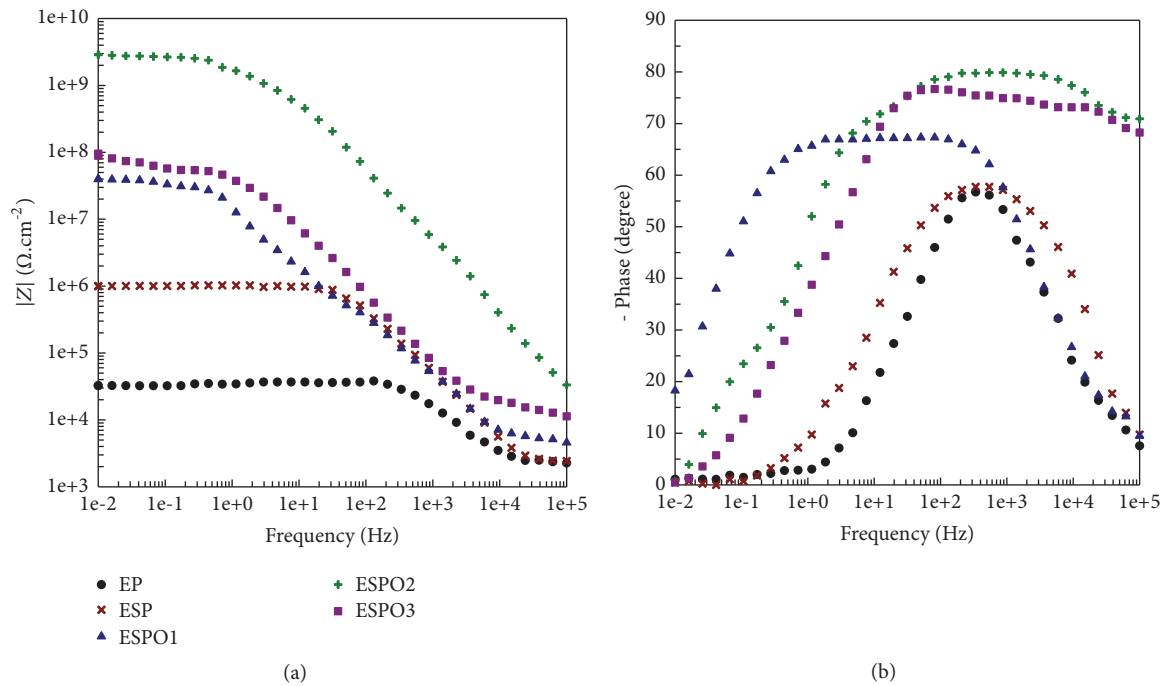


FIGURE 8: Bode plots of coatings after 14 days of immersion in 3% NaCl solution.

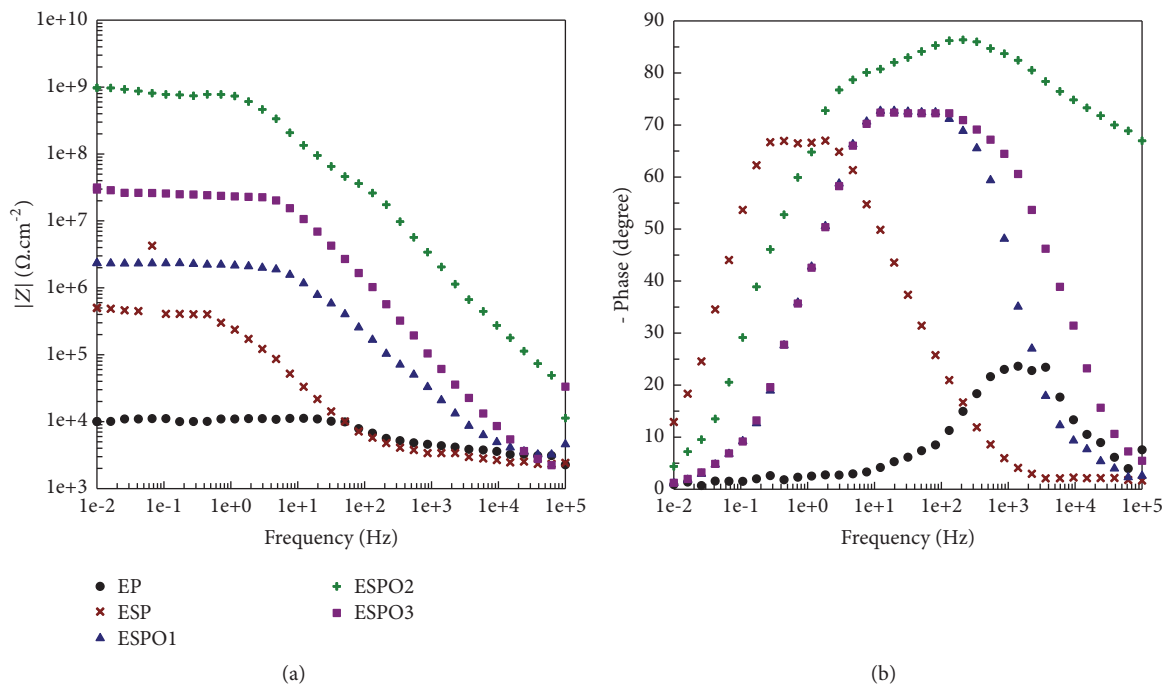


FIGURE 9: Bode plots of coatings after 35 days of immersion in 3% NaCl solution.

capacitive behavior with a high value of phase angle (higher than  $80^\circ$ ) in the middle frequency region. The capacity behavior in this region is reported that shows the insulating property of the surface coating. Furthermore, phase angles in low frequency results are quite important to measure the compactness of the coating. A very low phase angle occurred

for ESPO2 that demonstrates the existence of a compact coating with good corrosion resistance property. The results proved the efficiency of the oxalate anions addition to  $\text{SiO}_2/\text{PPy}$  for corrosion protection of steel surface.

Figure 10 plots  $|Z|_{100\text{mHz}}$  versus time for the carbon steel covered by pure epoxy coating and epoxy coatings

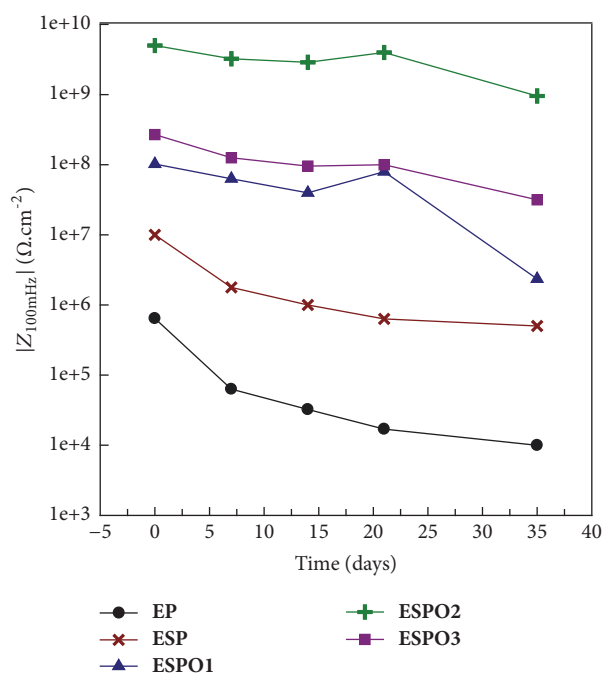


FIGURE 10:  $|Z|_{100\text{mHz}}$  versus immersion time in 3% NaCl solution of coatings.

containing composites SP, SPO1, SPO2, and SPO3. For all coatings,  $|Z|_{100\text{mHz}}$  values decreased during the first 14 days of test. This result indicates a rapid loss of the film protective properties due to the diffusion of aggressive ions. After this exposure time, the  $|Z|_{100\text{mHz}}$  values continued to decrease for the pure epoxy and epoxy containing composite  $\text{SiO}_2/\text{PPy}$ . For the epoxy coatings containing  $\text{SiO}_2/\text{PPyOx}$ , the  $|Z|_{100\text{mHz}}$  increased and decreased again after 21 days. As was widely reported, PPy is a smart conducting polymer which can prevent corrosion of steel in two different ways; PPy acts as a physical barrier in paint film which prevents penetration of corrosive ions across the coating. On the other hand, it passivates the surface of the steel substrate by the formation of iron oxides and iron complexes. As the counter anion, the release of oxalate anions affected directly the corrosion protection ability of the coating, which made the  $|Z|_{100\text{mHz}}$  increased again. After 35 days of exposure, the  $|Z|_{100\text{mHz}}$  value of epoxy coating containing SPO2 was higher than the  $|Z|_{100\text{mHz}}$  values of other coatings. The considerably high  $|Z|_{100\text{mHz}}$  value was obtained in the presence of oxalate anion in comparison with the one obtained without oxalate. It can be explained by the oxalate release from  $\text{SiO}_2/\text{PPyOx}$  at the steel surface. Oxalate can be released from  $\text{SiO}_2/\text{PPyOx}$  by the exchange reaction with anions like  $\text{Cl}^-$  and  $\text{OH}^-$ .

**3.8. Salt Spray.** Figure 11 shows some pictures of steel coated with epoxy coating, epoxy coating containing  $\text{SiO}_2/\text{PPy}$  and  $\text{SiO}_2/\text{PPyOx}$  after exposure to salt spray for 28 days. There are severe rusting and blistering along the scribe mark with EP. Furthermore, there are several pinholes on the coating surface. The loss of adherence of the epoxy coatings to its

substrate during prolonged exposure to the salt spray is indicated. It is due to the penetration of aggressive ions into the metal surface. In the case of ESP, less rusting and blistering are revealed. More interesting, the epoxy coating containing composites  $\text{SiO}_2/\text{PPyOx}$  shows no blister and corrosion products formed at scratches were limited. The salt spray test confirmed the best corrosion protection afforded by the ESPO2 coating, which match with the above results.

## 4. Conclusions

Composites  $\text{SiO}_2/\text{PPyOx}$  with different concentration of oxalate anion were synthesized successfully in situ. The electrochemical results indicated that the presence of oxalate anion significantly enhanced the effect of  $\text{SiO}_2/\text{PPy}$  on protection performance of epoxy coatings after 35 days of exposure to NaCl 3%. Such composites can be used as a promising inhibitor for organic coating to prevent corrosion and delay the degradation of steel exposed to high humidity and salt content conditions.

## Data Availability

The data used to support the findings of this study are available from the corresponding author upon request.

## Conflicts of Interest

The authors declare that they have no conflicts of interest.



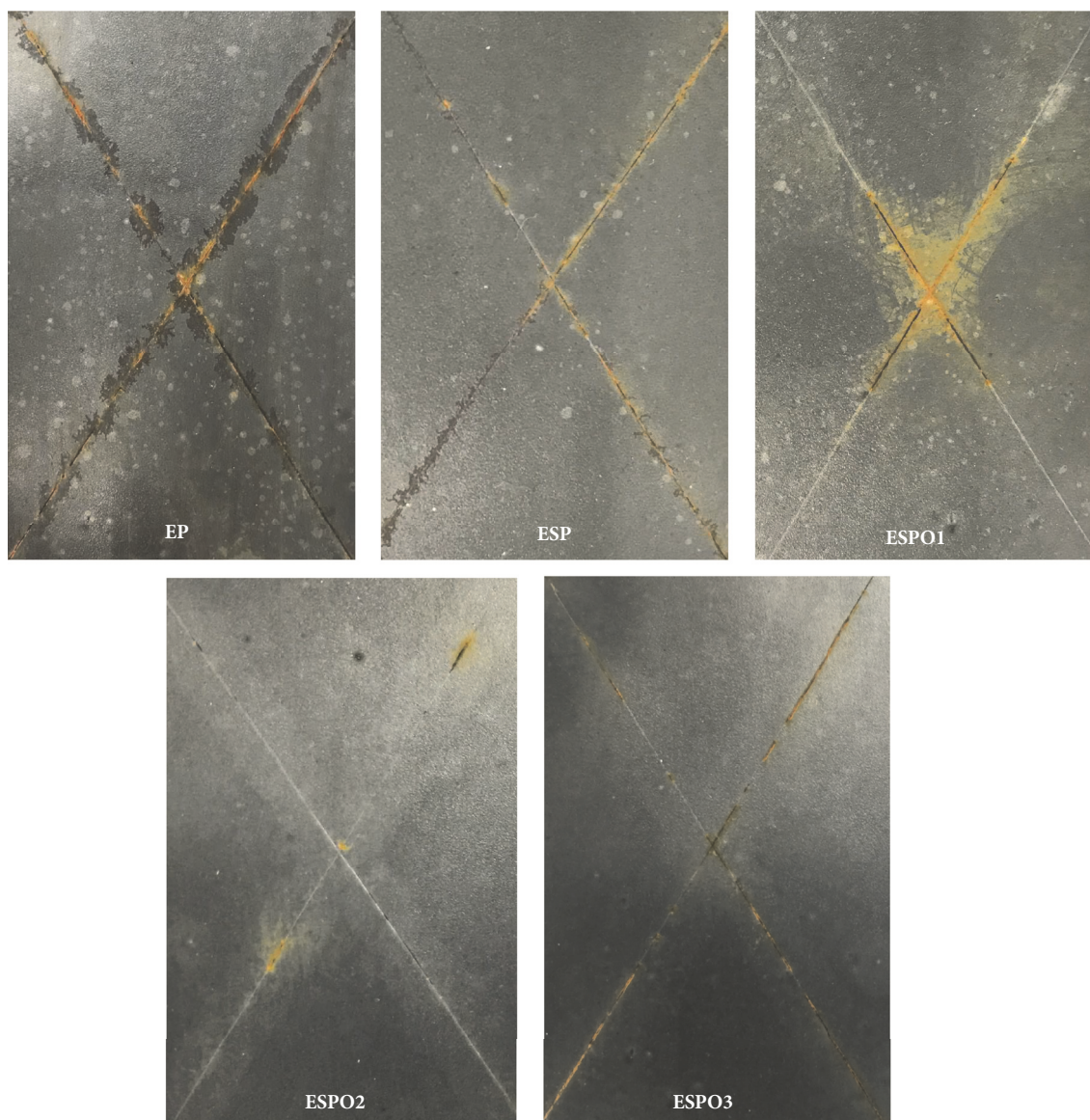


FIGURE 11: Photographs of coated steel panel exposed to salt spray for 28 days.

## Acknowledgments

This research was funded by Vietnam National Foundation for Science and Technology Development (NAFOSTED) under Grant no. [104.06-2014.12].

## References

- [1] M. Barletta, L. Lusvarghi, F. P. Mantini, and G. Rubino, "Epoxy-based thermosetting powder coatings: Surface appearance, scratch adhesion and wear resistance," *Surface and Coatings Technology*, vol. 201, no. 16-17, pp. 7479–7504, 2007.
- [2] H. Lee and K. Neville, *Handbook of Epoxy Resins*, McGraw Hill, New York, NY, USA, 1952.
- [3] J. Blasiak and J. Kowalik, "A comparison of the in vitro genotoxicity of tri- and hexavalent chromium," *Mutation Research - Genetic Toxicology and Environmental Mutagenesis*, vol. 469, no. 1, pp. 135–145, 2000.
- [4] E. Bakhshandeh, A. Jannesari, Z. Ranjbar, S. Sobhani, and M. R. Saeb, "Anti-corrosion hybrid coatings based on epoxy-silica nano-composites: Toward relationship between the morphology and EIS data," *Progress in Organic Coatings*, vol. 77, no. 7, pp. 1169–1183, 2014.
- [5] M. Conradi, A. Kocijan, D. Kek-Merl, M. Zorko, and I. Verpoest, "Mechanical and anticorrosion properties of nanosilica-filled epoxy-resin composite coatings," *Applied Surface Science*, vol. 292, pp. 432–437, 2014.
- [6] S. Sathiyarayanan, S. S. Azim, and G. Venkatachari, "A new corrosion protection coating with polyaniline-TiO<sub>2</sub> composite for steel," *Electrochimica Acta*, vol. 52, no. 5, pp. 2068–2074, 2007.
- [7] Z. Ranjbar, A. Jannesari, S. Rastegar, and S. Montazeri, "Study of the influence of nano-silica particles on the curing reactions of acrylic-melamine clear-coats," *Progress in Organic Coatings*, vol. 66, no. 4, pp. 372–376, 2009.
- [8] M. M. Jalili and S. Moradian, "Deterministic performance parameters for an automotive polyurethane clearcoat loaded

- with hydrophilic or hydrophobic nano-silica," *Progress in Organic Coatings*, vol. 66, no. 4, pp. 359–366, 2009.
- [9] A. J. Heeger, "Semiconducting and metallic polymers: The fourth generation of polymeric materials (nobel lecture)," *Angewandte Chemie International Edition*, vol. 40, no. 14, pp. 2591–2611, 2001.
  - [10] A. G. MacDiarmid, "Synthetic metals: a novel role for organic polymers (Nobel lecture)," *Angewandte Chemie International Edition*, vol. 40, no. 14, pp. 2581–2590, 2001.
  - [11] H. Shirakawa, "The discovery of polyacetylene film: the dawn of an era of conducting polymers (Nobel Lecture)," *Angewandte Chemie International Edition*, vol. 40, no. 14, pp. 2574–2580, 2001.
  - [12] A. Batool, F. Kanwal, M. Imran, T. Jamil, and S. A. Siddiqi, "Synthesis of polypyrrole/zinc oxide composites and study of their structural, thermal and electrical properties," *Synthetic Metals*, vol. 161, no. 23–24, pp. 2753–2758, 2012.
  - [13] M. R. Mahmoudian, Y. Alias, W. J. Basirun, and M. Ebadi, "Effects of different polypyrrole/TiO<sub>2</sub> nanocomposite morphologies in polyvinyl butyral coatings for preventing the corrosion of mild steel," *Applied Surface Science*, vol. 268, pp. 302–311, 2013.
  - [14] K. Qi, Y. B. Qiu, Z. Y. Chen, and X. P. Guo, "Corrosion of conductive polypyrrole: Galvanic interactions between polypyrrole and metal substrates," *Corrosion Science*, vol. 91, pp. 272–280, 2015.
  - [15] M. Saremi and M. Yeganeh, "Application of mesoporous silica nanocontainers as smart host of corrosion inhibitor in polypyrrole coatings," *Corrosion Science*, vol. 86, pp. 159–170, 2014.
  - [16] J. O. Iroh and W. Su, "Corrosion performance of polypyrrole coating applied to low carbon steel by an electrochemical process," *Electrochimica Acta*, vol. 46, no. 1, pp. 15–24, 2000.
  - [17] P. Ocón, A. B. Cristobal, P. Herrasti, and E. Fatas, "Corrosion performance of conducting polymer coatings applied on mild steel," *Corrosion Science*, vol. 47, no. 3, pp. 649–662, 2005.
  - [18] E. Armelin, R. Pla, F. Liesa, X. Ramis, J. I. Iribarren, and C. Alemán, "Corrosion protection with polyaniline and polypyrrole as anticorrosive additives for epoxy paint," *Corrosion Science*, vol. 50, no. 3, pp. 721–728, 2008.
  - [19] H. Nguyen Thi Le, B. Garcia, C. Deslouis, and Q. Le Xuan, "Corrosion protection and conducting polymers: Polypyrrole films on iron," *Electrochimica Acta*, vol. 46, no. 26–27, pp. 4259–4272, 2001.
  - [20] V. T. Van, T. T. Hang, P. T. Nam et al., "Synthesis of Silica/Polypyrrole Nanocomposites and Application in Corrosion Protection of Carbon Steel," *Journal of Nanoscience and Nanotechnology*, vol. 18, no. 6, pp. 4189–4195, 2018.
  - [21] L. M. Duc and V. Q. Trung, *Layers of Inhibitor Anion – Doped Polypyrrole for Corrosion Protection of Mild Steel*, INTECH, chapter 7, pp 143–174, 2013.
  - [22] C. Tohumcu, R. Taş, and M. Can, "Increasing the crystallite and conductivity of polypyrrole with dopant used," *Ionics*, vol. 20, no. 12, pp. 1687–1692, 2014.
  - [23] L. Ruangchuay, J. Schwank, and A. Sirivat, "Surface degradation of  $\alpha$ -naphthalene sulfonate-doped polypyrrole during XPS characterization," *Applied Surface Science*, vol. 199, no. 1–4, pp. 128–137, 2002.
  - [24] O. Grari, A. Et Taouil, L. Dhouibi et al., "Multilayered polypyrrole-SiO<sub>2</sub> composite coatings for functionalization of stainless steel: Characterization and corrosion protection behavior," *Progress in Organic Coatings*, vol. 88, pp. 48–53, 2015.
  - [25] G. Ruhi, O. P. Modi, and S. K. Dhawan, "Chitosan-polypyrrole-SiO<sub>2</sub> composite coatings with advanced anticorrosive properties," *Synthetic Metals*, vol. 200, pp. 24–39, 2015.
  - [26] B. N. Grgur, P. Živković, and M. M. Gvozdenović, "Kinetics of the mild steel corrosion protection by polypyrrole-oxalate coating in sulfuric acid solution," *Progress in Organic Coatings*, vol. 56, no. 2–3, pp. 240–247, 2006.
  - [27] Z. Chen, W. Yang, B. Xu et al., "Corrosion behaviors and physical properties of polypyrrole-molybdate coating electropolymerized on carbon steel," *Progress in Organic Coatings*, vol. 122, pp. 159–169, 2018.
  - [28] J. Wang, C. Wu, P. Wu, X. Li, M. Zhang, and J. Zhu, "Polypyrrole capacitance characteristics with different doping ions and thicknesses," *Physical Chemistry Chemical Physics*, vol. 19, no. 31, pp. 21165–21173, 2017.
  - [29] C. Merlini, B. S. Rosa, D. Müller, L. G. Ecco, S. D. A. S. Ramôa, and G. M. O. Barra, "Polypyrrole nanoparticles coated amorphous short silica fibers: Synthesis and characterization," *Polymer Testing*, vol. 31, no. 8, pp. 971–977, 2012.



